Control of Aggregation and Tuning of the Location of Porphyrins in Synthetic Membranes as Mimics for Cytochrome P450

A. P. H. J. Schenning, D. H. W. Hubert, M. C. Feiters,* and R. J. M. Nolte*

Department of Organic Chemistry, NSR Center, University of Nijmegen, Toernooiveld, 6525 ED Nijmegen, The Netherlands

Received June 19, 1995. In Final Form: December 9, 1995[⊗]

The aggregation and location of two series of tetraarylporphyrins in positively and negatively charged bilayers have been examined. Aggregation of the porphyrins can be reduced by introducing pyridinium groups on the porphyrin ring. In the positively charged bilayers, the degree of aggregation of the porphyrins increases with the number of charges on it. The opposite behavior is found in the case of negatively charged bilayers. All the charged porphyrins form face to face type aggregates whereas the uncharged ones form edge to edge type aggregates. Reduction of aggregation can also be achieved by using "picket-fence" type porphyrins which form head to tail aggregates. The location of the porphyrins in the bilayer is also investigated. The charged porphyrins are located near the aqueous interface and the uncharged ones in the hydrophobic part of the bilayer. Picket-fence porphyrin **7** was found to be the most promising candidate for being studied as a catalyst in cytochrome P450 mimics.

Introduction

Porphyrins play an important role in biological processes, *e.g.*, substrate oxidation reactions and conversion of light energy into chemical energy.[1,2] As part of our research program dealing with model systems for the membrane-bound enzyme system cytochrome P450, we are interested in the catalytic properties of porphyrins located in bilayers.[3,4] The active center of cytochrome P450 contains an iron porphyrin which is involved in oxygen binding and subsequent activation.[1] In the development of a membrane-bound mimic for this enzyme, it is important to evaluate the aggregation properties and the location of porphyrins within membranes. It has been found previously that aggregation can reduce the catalytic efficiency of a porphyrin, while its location in the membrane can determine its selectivity.[5,6]

We are using two strategies to prevent porphyrins from aggregating in our membrane-bound cytochrome P450 mimic.[4] The first is the use of sterically encumbered, so-called "picket-fence", porphyrins.[7] The second is the incorporation of positively charged porphyrins in negatively charged vesicles. Because of electrostatic interactions, these porphyrins will prefer to be surrounded by the negatively charged amphiphiles rather than by other positively charged porphyrins.

The location within the membrane can be tuned by using charged and uncharged porphyrins as we have shown elsewhere.[8] Charged porphyrins are preferentially bound near the surface of the bilayer, whereas uncharged ones are located in the center of the bilayer.

Chart 1

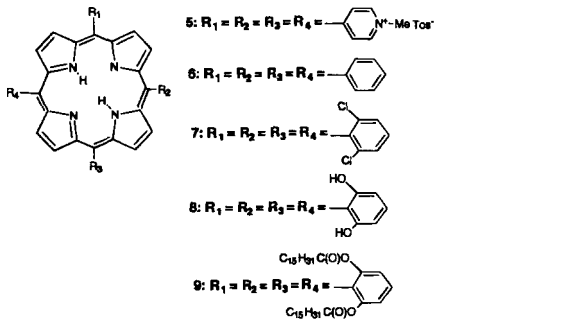

To date the aggregation and location properties of only a limited number of porphyrins in bilayers have been investigated. The studies reported sofar are aimed at mimicking photosynthetic proteins.[9–13] In this paper we report on the location and the aggregation properties of nine porphyrins (Chart 1) in synthetic surfactant vesicles derived from positively charged dioctadecyldimethylammonium chloride (DODAC) and negatively charged dihexadecyl phosphate (DHP) amphiphiles.[14]

Experimental Section

Instrumentation. ^{1}H NMR spectra were recorded on a Bruker WH90 (90 MHz) or a Bruker AM400 (400 MHz) spectrometer, at room temperature. Chemical shifts are given in ppm downfield from tetramethylsilane. Abbreviations used

⊗ Abstract published in *Advance ACS Abstracts*, February 15, 1996.

(1) Guengerich, F. P. *J. Biol. Chem.* **1991**, *266*, 10019.
(2) Zuber, H.; Brunisholz, R. A. *Chlorophyls*; Scheer, H., Ed.; CRC Press: Boca Raton, FL, 1991; pp 627–703.
(3) van Esch, J.; Roks, M. F.; Nolte, R. J. M. *J. Am. Chem. Soc.* **1986**, *108*, 6093.
(4) Schenning, A. P. H. J.; Hubert, D. H. W.; Feiters, M. C.; Nolte, R. J. M. *Angew. Chem.* **1994**, *106*, 2587; *Angew. Chem., Int. Ed. Engl.* **1994**, *33*, 2468.
(5) Tsuchida, E.; Nishide, H. *Top. Curr. Chem.* **1986**, *132*, 63.
(6) Groves, J. T.; Neumann, R. *J. Am. Chem. Soc.* **1989**, *111*, 2900.
(7) Nolte, R. J. M.; Razenberg, J. A. S. J.; Schuurman, R. *J. Am. Chem. Soc.* **1986**, *108*, 2751.
(8) van Esch, J.; Feiters, M. C.; Peters, A. M.; Nolte, R. J. M. *J. Phys. Chem.* **1994**, *98*, 5541.
(9) Chastenet de Castaing, E.; Kevan, L. *J. Phys. Chem.* **1991**, *95*, 10178.
(10) Lee, A. G. *Biochemistry* **1975**, *14*, 4397.
(11) Katagi, T.; Yamamura, T.; Saito, T.; Sasaki, Y. *Chem. Lett.* **1981**, 1451.
(12) Kang, S. K.; Kevan, L. *J. Phys. Chem.* **1994**, *98*, 4389.
(13) Takami, A.; Mataga, N. *J. Phys. Chem.* **1987**, *91*, 618.
(14) Carmona-Ribeiro, A. M. *Chem. Soc. Rev.* **1992**, 209.

0743-7463/96/2412-1572$12.00/0

are s = singlet, d = doublet, t = triplet, m = multiplet, and b = broad. Infrared and UV–vis spectra were obtained with a Perkin-Elmer 298 and a thermostated Perkin-Elmer Lambda 5 spectrophotometer, respectively. Fluorescence spectra were measured with a thermostated Perkin-Elmer MPF 4 fluorospectrometer. Transmission electron microscopy was carried out with a Philips EM 201 microscope. EPR spectra were recorded on a Bruker ESP 300 spectrometer, equipped with a Oxford flow cryostat.

Materials. For the preparation of the vesicles absolute ethanol, distilled tetrahydrofuran, and deionized water were used. DODAC was prepared from DODAB (*N,N*-dioctadecyl-*N,N*-dimethylammonium bromide) by ion exchange chromatography.[8] DHP, tris(hydroxymethyl)aminomethane (Tris), 4-pyridinecarbaldehyde, methyltosylate, and pyrrole were purchased from Aldrich. Pyrrole was freshly distilled before use. Thin-layer chromatography (TLC) was performed on precoated F-254 plates and column chromatography using basic alumina and silica 60H (from Merck).

5,10,15,20-Tetraphenylporphyrin (**6**), 5,10,15,20-tetrakis(2,6-dichlorophenyl)porphyrin (**7**), and 5,10,15,20-tetrakis(2,6-dihydroxyphenyl)porphyrin (**8**) were prepared according to literature procedures.[15–17] 4-(Hexadecyloxy)benzaldehyde was prepared as described in the literature.[18]

Synthesis of Porphyrins 1–5. Freshly distilled pyrrole (4 mL, 57 mmol) was slowly added under stirring to a solution of 4-(hexadecyloxy)benzaldehyde (5.1 g, 14 mmol) and 4-pyridinecarbaldehyde (4.5 mL, 42 mmol) in 240 mL of refluxing propionic acid. Refluxing was continued for 2 h, whereafter the propionic acid was evaporated, and the resulting solid was adsorbed on alumina. A mixture of porphyrins was isolated by flash chromatography (alumina, eluent $CHCl_3$). With subsequent column chromatography (silica, eluent $CHCl_3$/MeOH, 99.5/0.5) six fractions were obtained which could be identified as 5,10,15,20-(4-(hexadecyloxy)phenyl)porphyrin (**1**) (R_f($CHCl_3$/MeOH, 95/5 v/v) = 0.95), 5-(4-pyridyl)-10,15,20-tris(4-hexadecyloxy)phenyl)porphyrin (R_f($CHCl_3$/MeOH, 95/5, v/v) = 0.90), 5,15-bis(4-pyridyl)-10,20-bis(4-(hexadecyloxy)phenyl)porphyrin (R_f($CHCl_3$/MeOH, 95/5, v/v) = 0.65), 5,10-bis(4-pyridyl)-15,20-bis-(4-(hexadecyloxy)-phenyl)porphyrin (R_f ($CHCl_3$/MeOH, 95/5, v/v) = 0.45), 5,10,-15–tris(4-pyridyl)-20-(4-(hexadecyloxy)phenyl)porphyrin (R_f ($CHCl_3$/MeOH, 95/5, v/v) = 0.25), and 5,10,15,20-tetrakis(4-pyridyl)porphyrin (R_f ($CHCl_3$/MeOH, 95/5, v/v) = 0.05).

5,10,15,20-Tetrakis(4-(hexadecyloxy)phenyl)porphyrin (1). Yield: 220 mg (1.0%). ^{1}H-NMR (90 MHz, $CDCl_3$) δ: 8.8 (s, 8H, β-pyrrole), 8.0 (d, 8H, phenyl), 7.2 (d, 8H, phenyl), 4.2 (t, OCH_2), 2.2–1.1 (b, 126H, CH_2), 0.9 (t, 12H, CH_3), −2.5 (b, 2H, NH). FAB MS (matrix, nitrobenzyl alcohol): m/z = 1351 (M − $C_{16}H_{33}$). UV–vis (CH_2Cl_2) λ/nm, (log(ϵ/M^{-1}·cm^{-1})): 421 (5.6), 518 (4.2), 555 (4.1), 593 (3.7), 650 (3.9).

5-(4-Pyridyl)-10,15,20-tris(4-(hexadecyloxy)phenyl)porphyrin. Yield: 430 mg (2.3%). ^{1}H-NMR (90 MHz, $CDCl_3$) δ: 8.8 (m, 2H, pyridyl, 8H, β-pyrrole), 8.0 (m, 2H, pyridyl, 6H, phenyl), 7.2 (d, 6H, phenyl), 4.2 (t, 6H, OCH_2), 2.1–1.1 (b, 84H, CH_2), 0.9 (t, 9H, CH_3), −2.5 (b, 2H, NH). UV–vis (CH_2Cl_2) λ/nm, 421, 519, 554, 592, 649.

5,15-Bis(4-pyridyl)-10,20-bis(4-(hexadecyloxy)phenyl)-porphyrin. Yield: 180 mg (1.2%). ^{1}H-NMR (400 MHz, $CDCl_3$) δ: 9.02 (d, 4H, pyridyl, J = 5.60 Hz), 8.94 (d, 4H, β-pyrrole, J = 4.79 Hz), 8.79 (d, 4H, β-pyrrole, J = 4.80 Hz), 8.17 (d, 4H, pyridyl, 5.79 Hz), 8.10 (d, 4H, phenyl, J = 8.47 Hz), 7.29 (d, 4H, phenyl, J = 8.56 Hz), 4.26 (t, 4H, OCH_2, J = 6.49 Hz), 2.01–1.27 (b, 56H, CH_2), 0.88 (t, 6H, CH_3, J = 6.56 Hz), −2.82 (s, 2H, NH). UV–vis (CH_2Cl_2) λ/nm, 419, 516, 552, 591, 648.

5,10-Bis(4-pyridyl)-15,20-bis(4-(hexadecyloxy)phenyl)-porphyrin. Yield: 410 mg (2.6%). ^{1}H-NMR (400 MHz, $CDCl_3$) δ: 9.02 (d, 4H, pyridyl, J = 5.19 Hz), 8.94 (d, 2H, β-pyrrole, J = 4.76 Hz), 8.91 (s, 2H, β-pyrrole), 8.82 (s, 2H, β-pyrrole), 8.78 (d, 2H, β-pyrrole, J = 4.74 Hz), 8.15 (d, 4H, pyridyl, J = 5.53 Hz), 8.09 (d, 4H, phenyl, J = 8.42 Hz), 7.27 (d, 4H, phenyl, J = 8.47 Hz), 4.23 (t, 4H, OCH_2, J = 6.47 Hz), 2.01–1.19 (b, 56H, CH_2), 0.88 (t, 6H, CH_3, J = 6.42 Hz), −2.81 (s, 2H, NH). UV–vis (CH_2Cl_2) λ/nm, 420, 516, 552, 591, 647.

5,10,15-Tris(4-pyridyl)-20-(4-(hexadecyloxy)phenyl)porphyrin. Yield: 300 mg (2.5%). ^{1}H-NMR (90 MHz, $CDCl_3$) δ: 9.2 (m, 6H, pyridyl, 2H, β-pyrrole), 9.0 (s, 6H, β-pyrrole), 8.3 (d, 6H, pyridyl), 8.2 (d, 2H, phenyl), 7.5 (d, 2H, phenyl), 4.3 (t, 2H, OCH_2), 1.3–1.5 (b, 28H, CH_2), 0.8 (t, 3H, CH_3), −2.5 (b, 2H, NH). UV–vis (CH_2Cl_2) λ/nm, 418, 514, 549, 589, 646.

5,10,15,20-Tetrakis(4-pyridyl)porphyrin. Yield: 200 mg (2.3%). ^{1}H-NMR (90 MHz, $CDCl_3$) δ: 9.4 (d, 8H, pyridyl), 9.2 (s, 8H, β-pyrrole), 8.2 (d, 8H, pyridyl), −2.5 (b, 2H, NH). UV–vis (CH_2Cl_2) λ/nm, 416, 513, 546, 588, 643.

5-(1-Methyl-4-pyridyl)-10,15,20-tris(4-(hexadecyloxy)-phenyl)porphyrin Monotosylate (2). Under a nitrogen atmosphere, 100 mg of 5-(4-pyridyl)-10,15,20-tris(4-(hexadecyloxy)phenyl)porphyrin and 0.1 mL of methyl tosylate were dissolved in 10 mL of a mixture of toluene/acetonitrile (2/1, v/v). The reaction mixture was stirred at 80 °C for 16 h. After cooling to room temperature, the reaction mixture was poured over a glass filter filled with silica. After washing with 50 mL of CH_2Cl_2, compound **2** was isolated by elution with $CHCl_3$/MeOH, (9/1, v/v). Yield: 70 mg (61%) of **2** as a purple powder. ^{1}H-NMR (90 MHz, $CDCl_3$) δ: 9.5 (b, 2H, pyridyl), 8.8 (s, 8H, β-pyrrole), 8.6 (b, 2H, pyridyl), 8.1 (d, 2H, tosylate), 7.9 (d, 6H, phenyl), 7.3 (d, 3H, tosylate), 7.1 (d, 6H, phenyl), 5.0 (s, 3H, NCH_3), 4.2 (t, 6H, OCH_2), 2.2 (s, 3H, tosylate-CH_3), 2.1–1.1 (b, 84H, CH_2), 0.9 (t, 9H, CH_3), −2.5 (b, 2H, NH). FAB MS (matrix, nitrobenzyl alcohol): m/z = 1352 (M-Tos). UV–vis ($CHCl_3$/EtOH, 3/7) λ/nm (log(ϵ/M^{-1}·cm^{-1})): 424 (5.7), 522 (4.5), 568 (4.5), 584 (4.4), 657 (4.2).

5,10-Bis(1-methyl-4-pyridyl)-15,20-bis(4-(hexadecyloxy)-phenyl)porphyrin ditosylate (3). This porphyrin was synthesized starting from 5,10-bis(4-pyridyl)-15,20-bis(4-(hexadecyloxy)phenyl)porphyrin, as described for **2**, except that in this case 0.2 mL of methyl tosylate was used. Yield: 72 mg (54%) of **3** as a purple powder. ^{1}H-NMR (90 MHz, CD_3OD/$CDCl_3$, 1/1) δ: 9.5 (d, 4H, pyridyl), 9.2 (d, 4H, pyridyl), 8.9 (s, 8H, β-pyrrole), 8.3 (d, 4H, phenyl), 7.6 (d, 4H, phenyl), 7.3 (d, 4H, tosylate), 7.1 (d, 4H, tosylate), 4.9 (s, 9H, NCH_3), 4.3 (t, 4H, OCH_2), 2.2 (s, 6H, tosylate-CH_3), 1.3–1.5 (b, 28H, CH_2), 0.8 (t, 3H, CH_3), −2.5 (b, 2H, NH). FAB MS (matrix, nitrobenzyl alcohol): m/z = 1297 (M-Tos). UV–vis (DMF) λ/nm, (log(ϵ/M^{-1}·cm^{-1})): 420 (5.0), 518 (3.9), 552 (3.7), 588 (3.5), 646 (3.3).

5,10,15-Tris(1-methyl-4-pyridyl)-20-(4-(hexadecyloxy)-phenyl)porphyrin Tritosylate (4). This porphyrin was synthesized starting from 5,10,15-tris(4-pyridyl)-20-(4-(hexadecyloxy)phenyl)porphyrin, as described for **2**, except that in this case 0.3 mL of methyl tosylate was used. Yield: 90 mg (55%) of **4** as a purple powder. ^{1}H-NMR (90 MHz, CD_3OD) δ: 9.5 (d, 6H, pyridyl), 9.2 (d, 6H, pyridyl), 8.9 (s, 8H, β-pyrrole), 8.3 (d, 2H, phenyl), 7.6 (d, 2H, phenyl), 7.3 (d, 6H, tosylate), 7.1 (d, 6H, tosylate), 4.9 (s, 9H, NCH_3), 4.3 (t, 2H, OCH_2), 2.2 (s, 9H, tosylate-CH_3), 1.3–1.5 (b, 28H, CH_2), 0.8 (t, 3H, CH_3), −2.5 (b, 2H, NH). FAB MS (matrix, nitrobenzyl alcohol): m/z = 1246 (M-Tos). UV–vis (DMF) λ/nm (log(ϵ/M^{-1}·cm^{-1})): 418 (5.0), 522 (3.9), 552 (3.7), 587 (3.5), 645 (3.3).

5,10,15,20-Tetrakis(1-methyl-4-pyridyl)porphyrin Tetratosylate (5). This porphyrin was synthesized starting from 5,10,15,20-tetrakis(4-pyridyl)porphyrin, as described for **2**, except that in this case 0.6 mL of methyl tosylate was used and that the reaction was carried out in DMF as the solvent. Yield: 155 mg (71%) of **5** as a purple powder. ^{1}H-NMR (CD_3OD) δ: 9.4 (d, 6H, pyridyl), 9.2 (s, 8H, β-pyrrole), 9.0 (d, 6H, pyridyl), 7.6 (d, 6H, tosylate), 7.0 (d, 6H, tosylate), 4.9 (s, 12H, NCH_3), 2.2 (s, 12H, tosylate-CH_3), −2.5 (b, 2H, NH). FAB MS (matrix, nitrobenzyl alcohol): m/z = 1020 (M − 2Tos). UV–vis (MeOH) λ/nm, (log(ϵ/M^{-1}·cm^{-1})): 424 (5.6), 515 (4.4), 551 (4.0), 590 (4.0), 644 (3.5).

5,10,15,20-Tetrakis(2,6-dipalmitoylphenyl)porphyrin (9). To 25 mL of freshly distilled THF was added under a nitrogen atmosphere 200 mg (0.27 mmol) of 5,10,15,20-tetrakis(2,6-dihydroxyphenyl)porphyrin (**8**), 785 mg of palmitoyl chloride (2.85 mmol), and 325 mg (2.66 mmol) of (dimethylamino)pyridine. After stirring at room temperature for 24 h, the solvent was evaporated, dichloromethane was added, and the organic layer was washed twice with 2 N HCl and with sodium hydrocarbonate. The dichloromethane solution was dried ($NaSO_4$), filtered, and evaporated under reduced pressure. Further purification was achieved by column chromatography on silica with chloroform/

(15) Adler, A. D.; Longo, F. R.; Finarelli, J. D.; Goldmacher, J.; Assour, J.; Korsakoff, L. *J. Org. Chem.* **1967**, *32*, 476.
(16) Van der Made, A. W.; Nolte, R. J. M.; Drenth, W. *Recl. Trav. Chim. Pays-Bas* **1988**, *107*, 15.
(17) Tsuchida, E. *J. Chem. Soc., Dalton Trans.* **1990**, 2713.
(18) Gray, G. W.; Jones, B. *J. Chem. Soc.* **1954**, 1467.

diethyl ether (10/1, v/v) as the eluent. Yield: 90 mg (13%) of **9** as a purple powder. R_f($CHCl_3$/Et_2O, 10/1, v/v) = 0.83. ^{1}H-NMR ($CDCl_3$) δ: 8.9 (s, 8H, β-pyrrole), 9.0 (m, 12H, phenyl) 1.1−2.1 (m, 224H, CH_2), 1.0 (t, 24H, CH_3), −2.8 (b, 2H, NH). FAB MS (matrix, nitrobenzyl alcohol): m/z = 2650 (M). UV-vis ($CHCl_3$) λ/nm, (log(ϵ/M^{-1}·cm^{-1})): 417 (5.5), 510 (4.3), 586 (3.7), 652 (3.3).

Copper 5,10,15,20-Tetrakis(2,6-dichlorophenyl)porphyrin (Cu-7). 5,10,15,20-Tetra(2,6-dichlorophenyl)porphyrin (120 mg, 0.14 mmol) and 120 mg (0.55 mmol) of $Cu(OAc)_2$·$2H_2O$ were dissolved in 25 mL of DMF and refluxed until all free-base porphyrin was consumed (2.5 h, followed by UV−vis). After cooling to room temperature the reaction mixture was poured into water and extracted with 30 mL of CH_2Cl_2. The organic layer was washed twice with 50 mL of 5 wt % aqueous sodium carbonate solution. The organic layer was dried (Na_2SO_4), concentrated *in vacuo*, and subjected to column chromatography (silica, eluent MeOH/$CHCl_3$, 1/10, v/v). Yield: 99 mg (91%) of **Cu-7** as a purple powder. FAB MS (matrix, nitrobenzyl alcohol): m/z=951 (M). UV−vis ($CHCl_3$) λ/nm (log(ϵ/M^{-1}·cm^{-1})): 415 (5.6), 540 (4.2), 576 (3.6).

Vesicle Preparation. Aliquots of stock solutions of porphyrin and surfactant, calculated to give the desired concentrations, were mixed in a test tube. The solvent was evaporated under a stream of nitrogen to give a homogeneous thin film of porphyrin and surfactant. The film was dissolved in 100 μL of ethanol/THF (1/2, v/v). In the case of DODAC as surfactant, 50 μL of the solution was injected into 5 mL of water of 55 °C, while vortexing. In the case of DHP, the 50 μL solution was injected into 5 mL of Tris buffer solution (75 °C), which consisted of a 20 mM Tris solution adjusted to pH 7.8 with hydrochloric acid.

Incorporation Experiments. The incorporation efficiency was measured by gel permeation chromatography (GPC) in combination with fluorescence and UV−vis spectroscopy. Vesicle solutions prepared as described above (R = 1000, [porphyrin] = 1×10^{-6} M) were passed over a Sephadex G50 column with water (in the case of DODAC vesicles) or 20 mM Tris buffer (pH = 7.0, DHP vesicles) as the eluents. The fractions were collected and the fluorescence intensity and the absorption spectrum were measured to calculate the porphyrin and amphiphile concentrations.

Fluorescence Measurements. Quenching experiments were carried out with a thermostated cuvette at 75 and 65 °C for DHP and DODAC vesicles, respectively. For the self-quenching experiments, samples were prepared with different [amphiphile]/[porphyrin] ratios (R). The concentration of the porphyrins was 1×10^{-6} M in all cases. The porphyrin B-band was chosen as excitation wavelength (Table 1, highest R value). Quenching of the fluorescence with hydrophilic quenchers was studied by titrating 0.8 mL of a vesicle solution (R = 2000, [porphyrin] = 1×10^{-6} M) with 5 μL aliquots of a 20 mM NaI solution when using DODAC vesicles. Quenching titration experiments with negatively charged vesicles were carried out by adding 1 μL aliquots of a 30 mM $Cu^{II}SO_4$ solution to the vesicle solution. In this case, sodium dihexadecyl phosphate (NaDHP) was used instead of protonated DHP because aggregates formed by this amphiphile were found to be stable against copper(II) sulfate. The fluorescence intensity was measured 3 min after each addition of quencher and the data were corrected for volume increments.

Electron Microscopy. For the visualization of the vesicles the negative staining method was used. A droplet of a sample was placed on a carbon coated copper grid. The grids were first made hydrophilic by exposure to an argon plasma for 2 min. After allowing to adsorb on the grids for 2 min, the solution was drained with filter paper and the samples were stained with an aqueous uranyl acetate solution (1 wt %) which was removed after 1 min.

Fitting of the Self-Quenching Curves. The relation between the porphyrin concentration in the bilayer and the ratio R is as follows

$$[\text{porphyrin}]_{\text{total}} = (1/R)[\text{amphiphile}]_{\text{total}} \quad (1)$$

where the concentrations are related to the aqueous bulk. For the molar amount of porphyrin and the volume of the bilayer, the following relationships hold

$$\text{moles of porphyrin} = V_{\text{total}}[\text{porphyrin}]_{\text{total}} \quad (2)$$

$$V_{\text{bilayer}} = \alpha V_{\text{total}}[\text{amphiphile}]_{\text{total}} \quad (3)$$

where α is the molar volume of the amphiphile and V_{total} is the volume of the solution.

$$[\text{porphyrin}]_{\text{bilayer}} = \frac{\text{moles of porphyrin}}{V_{\text{bilayer}}} = \frac{V_{\text{total}}[\text{porphyrin}]_{\text{total}}}{\alpha V_{\text{total}}[\text{amphiphile}]_{\text{total}}} = \frac{1}{\alpha R} \quad (4)$$

Equation 4 gives the relationship between the porphyrin concentration in the bilayer and the ratio R. The fluorescence curves could be fitted by assuming the following equilibrium

$$n\text{M} \rightleftharpoons \text{A} \quad \text{with} \quad K_a = [\text{A}]/[\text{M}]^n \quad (5)$$

in which n is the aggregation number, M is the monomeric porphyrin, and A is the aggregate which is built up of n monomers. K_a is the association constant. For the total porphyrin concentration $[\text{porphyrin}]_{\text{bilayer}}$ we can write

$$[\text{porphyrin}]_{\text{bilayer}} = [\text{M}] + n[\text{A}] = [\text{M}] + nK_a[\text{M}]^n \quad (6)$$

If we assume that only monomeric porphyrins display fluorescence, we can write:

$$[\text{M}] = \Psi F \quad (7)$$

where F is the fluorescence intensity and Ψ is the instrument factor. This factor only depends upon the temperature and the instrument used but is constant during a series of measurements. If we combine eqs 5, 6, and 7, we can write

$$[\text{porphyrin}]_{\text{bilayer}} = \Psi F + nK_a[\Psi F]^n \quad (8)$$

This relation enables us to determine the aggregation number and the association constant from our fluorescence data. F can be substituted by $F/\alpha R$ in formula 8. This substitution of F enables comparison of the data, since this corrected fluorescence intensity is now related to the same volume of the bilayer. For the molar volume of both DODAC and DHP a concentration of 1.1 L/mol was taken.[8]

EPR Measurements. Vesicle dispersions (5 mL) of DHP or DODAC (5 mM) containing **Cu-7** (125 nM) were prepared by the modified ethanol injection method. These dispersions were dried on a Mylar film in a desiccator over sodium hydroxide or phosphorus pentoxide. The resulting films were carefully cut into 3 × 15 mm strips. Approximately 15 to 25 strips were stacked on a quartz rod and fixed with Sellotape. This rod was subsequently placed in the EPR spectrometer. The angle could be set by a goniometer.

Results

Incorporation. Efficient incorporation of porphyrins in bilayers of DODAC can usually be achieved by the ethanol injection method.[8] This method was also used for our porphyrins. The actual incorporation into the DODAC and DHP bilayers was checked by gel permeation chromatography (GPC). The GPC elution profiles showed that the elution volumes of DHP vesicles with porphyrins are the same as those of vesicles without porphyrins. Separate experiments revealed that nonincorporated porphyrins eluted much slower or not at all. In the case of DODAC vesicles, the same results were obtained. All porphyrins were incorporated quantitatively, with the exception of porphyrin **5**, which could not be efficiently incorporated in a DODAC membrane (less than 10% incorporation was detected by UV−vis spectroscopy). Electron micrographs of the eluted dispersions showed that closed spherical vesicles were present. The average diameter of the DODAC and DHP vesicles containing the porphyrins was 4000 Å. This diameter was the same for vesicles without porphyrins.

Table 1. Spectroscopic Data of Porphyrins in DODAC and DHP Bilayers

porphyrin, amphiphile	R	B band (λ_{max}, nm)	fluorescence (λ_{max}, nm)	
1, DODAC[a]	2000	421[b]	652	717
	200	402, 436		
DHP	2000	420	660	720
	200	400–440		
2, DODAC[a]	2000	426	660	720
	200	424		
DHP	2000	427	666	723
	200	427		
3, DODAC	2000	424	660	715
	200	422		
DHP	2000	427	665	716
	200	427		
4, DODAC	2000	423	660	714
	200	422		
DHP	2000	427	663	*c*
	200	427		
5, DODAC	2000	424	650	700
	200	422		
DHP	2000	427	660	718
	200	427		
6, DODAC[a]	2000	418	652	717
	200	420		
7, DODAC	8000	426	655	715
	50	444		
8, DODAC	8000	417	655	712
	50	428		
9, DODAC	8000	417	660	714
	50	424		

[a] Data taken from ref 8. [b] B band of **1** in hexane, $\lambda_{max} = 418$ nm; dichloromethane, $\lambda_{max} = 421$ nm; pyridine, $\lambda_{max} = 425$ nm. [c] Not determined.

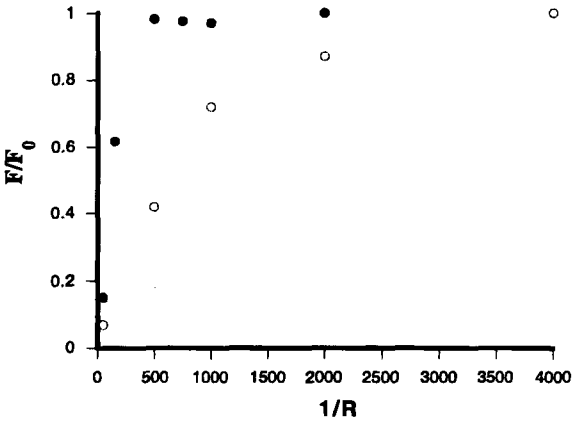

Figure 1. Self-quenching of the fluorescence of **4** in DODAC (○) vesicles and DHP (●) vesicles. F_0 is the fluorescence intensity at $R = 4000$.

Aggregation. In Table 1 the spectroscopic data of the porphyrins at two lipid/porphyrins ratios (R) are given. Upon going to a lower R only the B band is shifted, whereas the Q bands of all the porphyrins remain unchanged. The most likely explanation for this behavior is that the porphyrins tend to aggregate as the lipid/porphyrin ratio decreases. When the porphyrins are aggregated, a strong exciton coupling will exist which can cause a shift of the B-band.[20]

Figures 1 and 2 show examples of the effect of changing the lipid/porphyrin ratio on the fluorescence intensity, while keeping the amount of porphyrin constant. In the case of the charged porphyrins the most pronounced fluorescence differences were observed for **4** in DODAC and DHP vesicles. In the "picket-fence" series the most

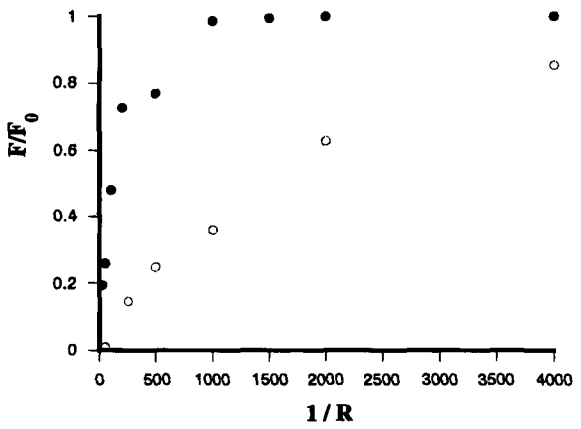

Figure 2. Self-quenching of the fluorescence of **6** (○) and **7** (●) in DODAC vesicles. F_0 is the fluorescence intensity at $R = 4000$.

Table 2. Aggregation Data for Porphyrins in DODAC and DHP Bilayers

porphyrin, amphiphile	R[a]	n[b]	K_a[c] ($M^{-(1-n)}$)
1, DODAC	2000	9.2[d]	5.6×10^{28} [d]
DHP	2000		
2, DODAC	300	2.8	1.4×10^4
DHP	150	2.7	3.1×10^4
3, DODAC	450	2.7	3.5×10^4
DHP	150	3.0	2.9×10^4
4, DODAC	600	4.4[d]	4.3×10^{11} [d]
DHP	150	2.9	1.3×10^4
5, DODAC	700	6.9[d]	5.2×10^{18} [d]
DHP	150	2.8	9.5×10^3
6, DODAC	1500	6.0[d]	1.0×10^{14} [d]
7, DODAC	120	2.0	6.5×10^3
8, DODAC	1100	2.1	4.6×10^5
9, DODAC	270	3.2	2.2×10^4

[a] Ratio where $F_0/F = 2$. [b] Aggregation number. [c] Association constant. [d] These values are inaccurate because the determination could not be carried out in the range recommended[29] for such high association constants due to problems with the fluorescence yield.

pronounced differences were found between **6** and **7** in DODAC vesicles (Figure 2). When R decreases, the fluorescence intensity at a constant porphyrin concentration also decreases, which points to aggregation of the porphyrins.[19,20] In Table 2 the lipid/porphyrin ratios are given at which the fluorescence intensity is half that of the porphyrins in the monomeric form, i.e., the value at high lipid/porphyrin ratio. It was possible to fit the fluorescence curves with the help of formula 8 and to get values for the equilibrium constants and the aggregation numbers. The results are listed in Table 2. The estimated errors in the aggregation numbers and the association constant are 10%–50%.

Location. Quenchers can give information about the location of porphyrins in bilayers.[22] For quenching to occur a close contact must exist between the chromophore and the quenching compound. Hydrophilic quenchers will detect porphyrins that are located at the water–bilayer interface. Porphyrins which are located in the inner part of the membrane will not be quenched by these compounds. We used iodide ions as quenchers in the case of DODAC vesicles, because these ions will adsorb strongly to the quaternary ammonium groups of these aggregates. In the case of DHP vesicles, we used copper ions. The quenching experiments were carried out above the phase

(19) Richelli, F.; Jori, J. *Photochem. Photobiol.* **1986**, *44*, 151.
(20) Margalit, R.; Shaklai, N.; Cohen, S. *Biochem. J.* **1983**, *209*, 547.
(21) Kasha, R.; Rawls, H. R.; Asraf El-Bayoumi, M. *Pure Appl. Chem.* **1965**, *11*, 371.
(22) Radda, G. K.; Vanderkooi, J. *Biochim. Biophys. Acta* **1972**, 265.

Table 3. Stern–Volmer Quenching Constants (K_{SV}) for Various Combinations of Porphyrins and Hydrophilic Quenchers in DODAC and DHP Vesicles

porphyrin	NaI/DODAC K_{SV} (M^{-1})	$Cu^{II}SO_4$/DHP K_{SV} (M^{-1})
1	478	
2	4570	4142
3	10700	4020
4	4420	3410
5	2100	4986
6	430[a]	
7	80	
8	−581[b]	
9	17	

[a] Data taken from ref 8. [b] Stern–Volmer constants measured in $CHCl_3$ and MeOH amount to −40 and 230, respectively.

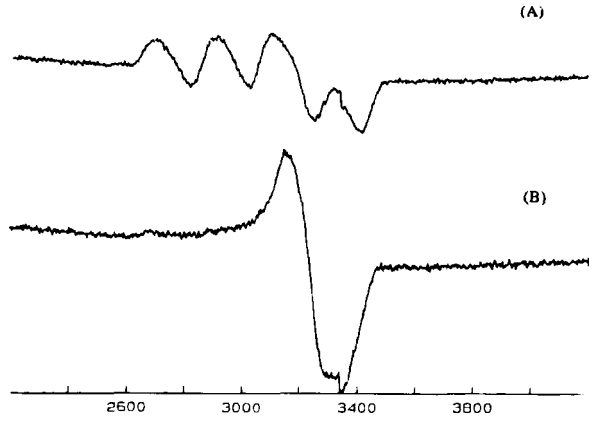

Figure 3. EPR spectra of **Cu-7** in DHP bilayers (R = 200) measured at two different orientations (see text); (A) magnetic field parallel to the bilayer normal; (B) magnetic field perpendicular to the bilayer normal.

transition temperature of the vesicles. Linear Stern–Volmer plots were obtained up to a quencher concentration of 10% of the amphiphile concentration. The obtained Stern–Volmer constants are given in Table 3. These constants are not corrected for partition of the quencher between the aqueous phase and the vesicle phase nor for the possibilities that vesicle fusion occurs or that osmotic effects induced by the quenchers take place.[28]

Orientation. The orientation of the porphyrins in the DHP and DODAC bilayers was investigated by EPR spectroscopy using the copper(II) derivate of porphyrin **7** as the model compound. Aligned bilayers were obtained by allowing a vesicular solution of **Cu-7** to dry on a flat support, i.e., Mylar.[23] These so-called "cast bilayers" are regulary stacked with the porphyrin planes parallel to the surface. The square planar porphyrin ligand around the copper(II) nucleus gives rise to a strong anisotropy of both the **g**-tensors and the $\mathbf{A}^{Cu}$ tensors. Incorporation in oriented bilayers and subsequent measurements of EPR spectra at various angles between the bilayer and the magnetic field gives information about the orientation of the porphyrin.[24,25] The orientation-dependent EPR spectra (Figure 3) were measured at angles of $\alpha = 0°$ and $\alpha = 90°$ (α is the angle between the bilayer normal and the magnetic field). In order to describe this orientation, a coordinate system was defined as discussed previously.[8] At $\alpha = 0°$, a spectrum with four lines ($A_{\parallel}^{Cu} = 210$ G, $g_{eff} = 2.201 = g_{\parallel}$) and at $\alpha = 90°$ a spectrum with one line ($g_{eff} = 2.061 = g_{\perp}$) was measured. The EPR spectrum of **Cu-7** in a frozen $CHCl_3$ glass was also recorded ($g_{\perp} = 2.066$, $g_{\parallel} = 2.191$ and $A_{\parallel}^{Cu}/G = 207$, $A_{\perp}$ was not resolved). This powder spectrum did not reveal any nitrogen hyperfine splitting which can be attributed to dipolar broadening, a phenomenon that can occur when two copper nuclei are as far apart as 20 Å.[26,27]

Discussion

Our incorporation experiments show that all porphyrins can successfully be incorporated in both DODAC and DHP vesicles, except **5** which cannot be anchored to DODAC vesicles. This latter behavior can be attributed to the fact that the four positively charged pyridyl groups of **5** prefer to be located in water rather than in the hydrophobic bilayer. In the case of DHP, this positively charged porphyrin probably is strongly adsorbed to the negatively charged surface of the vesicles. The measured diameter of 4000 Å is typical for vesicles prepared by the injection method and this diameter remains unaffected after incorporation of the porphyrins.[14]

At high amphiphile/porphyrin ratios (R), the porphyrins are not aggregated in the bilayers, as can be concluded from the fact that the fluorescence of these molecules is not quenched under these conditions (Figures 1 and 2). In the charged porphyrins series (**1**–**5**), going to low R values, aggregation is reduced if one or more charged pyridyl groups are introduced (see Table 2, aggregation numbers and association constants for **1** versus **2**–**5**). The self-quenching curves of the positively charged porphyrins show that in DODAC vesicles aggregation increases when the number of charges on the porphyrin unit becomes larger. This contrasts with the behavior of these porphyrins in DHP vesicles. In the latter negatively charged systems the aggregation decreases when going from porphyrin **2** to **5**. This trend is, however, less pronounced than the increase in aggregation observed for DODAC vesicles. These observations are in line with the amphiphile/porphyrin ratios (R) where $F_0/F = 2$ (Table 2). These ratios (R) remain almost the same in DHP vesicles but increase in the case of DODAC vesicles when going from porphyrin **2** to **5**. The behavior of the charged porphyrins in DHP vesicles can be explained in terms of electrostatic interactions between the porphyrins and the lipids. For this reason, the porphyrin with the greatest number of charged pyridyl groups is expected to have the lowest association constant, as borne out by the results (Table 2). In the case of DODAC vesicles electrostatic interactions play a less pronounced role and other factors become important. In these vesicles the aggregation increases when the number of tails decreases. Langmuir–Blodgett films formed by our amphiphilic porphyrins also show such behavior.[28] In these monolayers the organization of the porphyrins is largely determined by the balance between π–π interactions, the interaction of the hydrophilic head groups with the aqueous surface, and the sterical repulsion between the hydrocarbon chains. These factors apparently also play a role in our systems.

The absorption spectra of the porphyrins change when the ratio between porphyrin and amphiphile is varied. These changes can be interpreted by the exciton model developed by Kasha.[21] This theory predicts in a qualitative way the interactions between localized transition dipole moments. These interactions can cause a splitting of absorption bands. For an aggregate, the transition energy (E) is related to the energy of the monomer ($E_{monomer}$)

(23) Nashima, N.; Ando, R.; Kunitake, T. *Chem. Lett.* **1983**, 1577.
(24) Ishikawa, Y.; Kunitake, T. *J. Am. Chem. Soc.* **1991**, *113*, 612.
(25) Michalli, S.; Hugerat, M.; Levanon, H.; Bernitz, M.; Natt, A.; Neumann, R. *J. Am. Chem. Soc.* **1992**, *114*, 3612.
(26) Smith, T. D.; Pilbrow, J. R. *Coord. Chem. Rev.* **1974**, *13*, 173.
(27) Palmer, G. *Biochem. Soc. Trans.* **1985**, 548.
(28) Kroon, J. M.; Sudhölter, E. J. R.; Schenning, A. P. H. J.; Nolte, R. J. M. *Langmuir* **1995**, *11*, 214.
(29) Carta, G.; Crisponi, G. *J. Chem. Soc., Perkin Trans. 2* **1982**, 53.

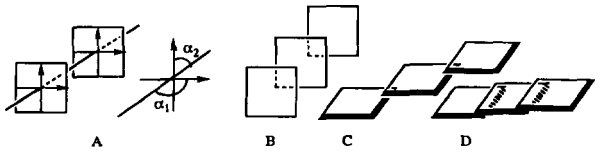

Figure 4. (A) Possible arrangements of porphyrins in aggregates. Definition of α_1 and α_2, the angles between the axis through the porphyrin centers and the two transition dipole moments. (B) Face-to-face type aggregate ($\alpha_1 = \alpha_2 = \pi/2$, blue shift of B-band). (C) Head-to-tail type aggregate ($\alpha_1 = \alpha_2 = \pi/4$, red shift of B-band). (D) Edge-to-edge type aggregate ($\alpha_1 = 0$, $\alpha_2 = \pi/2$, splitting of B-band).

according to the following equation:

$$E = E_{\text{monomer}} + D \pm \epsilon \qquad (9)$$

where D is the dispersion energy and ϵ is the exciton splitting. For N cofacially arranged chromophores, ϵ is related to the transition dipole moment (M), the center to center distance of these chromophores (R) and the angle α between the center to center vector and the transition moment

$$\epsilon = [2(N - 1/N)(M^2/R^3)(1 - 3\cos^2\alpha)] \qquad (10)$$

One of the two transitions is symmetry forbidden which usually results in only one absorption band. In porphyrins, however, the excited state is 2-fold degenerated with two dipole moments aligned at an angle of 90° along the axis through the pyrrole nitrogens at opposite positions in the porphyrin molecule. The absorption spectra of the porphyrins can therefore be explained in terms of the displacement of the molecules in aggregates along these axes (Figure 4). Porphyrin **1** displays the same behavior in DHP and DODAC vesicles.[8] The splitting of its B band suggests that edge to edge type aggregates are formed. The charged porphyrins show small blue shifts of the B band upon aggregation in DODAC vesicles, which indicates that "face to face" aggregates are present. This means that electrostatic repulsion between the positively charged porphyrins plays a less important role in the aggregate. The B band becomes red shifted upon going from DODAC to DHP vesicles. This suggests an electrostatic interaction between the cationic porphyrins and the anionic DHP amphiphiles.[12]

The "picket-fence" porphyrins were only studied in DODAC vesicles. The aggregation of these molecules increases in the order **7** > **9** > **8** > **6**, which implies that the substituents on the "picket-fence" porphyrins reduce aggregation. Acylation of **8** to give porphyrin **9** results in a decrease in aggregation number. The presence of intermolecular hydrogen bonds (see below) can be an explanation for the fact that **8** aggregates more strongly than **9**. Porphyrin **7** results in a decrease in aggregation number. The presence of intermolecular hydrogen bonds (see below) can be an explanation for the fact that **8** aggregates more strongly than **9**. Porphyrin **7** was found to have the lowest aggregation number ($R = 120$ where $F_0/F = 2$) of all nine porphyrins. All "picket-fence" porphyrins showed a red shift of the B band with decreasing amphiphile/porphyrin ratio (R), which according to the exciton theory suggests that "head to tail" type aggregates are formed. For sterical reasons the porphyrins probably cannot form face to face type aggregates. The red shift is the largest for **7** which indicates that the porphyrin molecules in this aggregate have a strong interaction energy.

The Stern–Volmer quenching constants measured for our porphyrins show that the location of these molecules in the bilayers depends on the nature of the substituents on the porphyrin rings. The general trend is that the porphyrins move to a region in the bilayer that is compatible with their polarity. The charged porphyrins are located near the interface (highest Stern–Volmer quenching constant) whereas the porphyrins without hydrophilic substituents are situated more in the inner part of the bilayer. The location of the latter porphyrins probably is between the bilayer center and the interface, as can be concluded from the fact that the absorption maximum of the B band of porphyrin **1** in the bilayers is almost the same as that in a solvent of intermediate polarity, *i.e.*, dichloromethane (Table 1, footnote *b*). Similar effects were also found in the case of the other uncharged porphyrins. The negative Stern–Volmer constant measured for **8** can be explained in terms of the presence of hydrogen bonds which results in the formation of nonfluorescent aggregates. In methanol, **8** is not aggregated and a normal Stern–Volmer constant is found. In chloroform intermolecular hydrogen bonds between the porphyrins are possible and aggregates are present. Upon the addition of iodide ions these interactions break down resulting in an increase in fluorescence. This effect is probably stronger than the quenching. The negative quenching value in DODAC vesicles can be caused by the same behavior as found in chloroform. The strong effect of iodide on the fluorescence of **8** suggests that this porphyrin is located near the interface.

Porphyrin **7** gives typical EPR spectra for a porphyrin with a orientation perpendicular to the bilayer normal. It is interesting that for DHP and DODAC amphiphiles well-defined bilayers could be obtained in contrast with earlier findings.[8] The orientation of porphyrin **7** in DODAC is different from that found for porphyrin **6** ($\alpha = 30°$). An explanation for this result can be that **6** ($R = 200$; 85% aggregated, $K = 1 \times 10^{14}$) aggregates more strongly than **7** ($R = 200$; <40% aggregated, $K = 6.5 \times 10^3$). So for **6** the orientation of a porphyrin aggregate is measured, whereas in the case of **7** it is for a porphyrin monomer.

Considering the aggregation and location properties, porphyrin **7** is probably the most promising candidate to study as a catalyst in cytochrome P450 mimics. This porphyrin could give the highest catalytic efficiency because the aggregation of this porphyrin in the bilayer is strongly reduced, due to the ortho substituents on the phenyl ring. The location of **7** in the hydrophobic part of the bilayer is analogous to the environment of the catalytic center found in the natural system.

Acknowledgment. This work was supported by the Netherlands Foundation for Chemical Research (SON) with financial aid from The Netherlands Organization for Scientific Research (NWO). The authors thank Dr. J. H. Van Esch for stimulating discussions, and G. E. Janssen and A. A. K. Klaasen for help with the EPR measurements.

LA950486A